Original Article

# Evaluation of the tumoricidal efficacy of adoptive cell transfer using hepatocellular carcinoma-derived organoids

**Zizhen Zhou[1#], Xiaoluan Yan[2#], Wanwan Shi[1], Kangan Tan[1], Chen Shao[3], Yan Wang[1], Guiqiang Wang[1], Yuan Hong[1]^**

[1]Infectious Diseases Department, Peking University First Hospital, Beijing, China; [2]General Surgery Department, Beijing Cancer Hospital, Beijing, China; [3]Pathology Department, Capital Medical University Youan Hospital, Beijing, China

*Contributions:* (I) Conception and design: Y Hong; (II) Administrative support: G Wang; (III) Provision of study materials or patients: X Yan, C Shao; (IV) Collection and assembly of data: Z Zhou, X Yan; (V) Data analysis and interpretation: W Shi, K Tan, Y Wang; (VI) Manuscript writing: All authors; (VII) Final approval of manuscript: All authors.

[#]These authors contributed equally to this work.

*Correspondence to:* Yuan Hong. 8 Xishiku Street, Beijing 100034, China. Email: hongy@bjmu.edu.cn.

**Background:** Tumor-derived organoid, namely tumoroid, can realistically retain the clinicopathologic features of original tumors even after long-term *in vitro* expansion. Here we develop this production methodology derived from hepatocellular carcinoma primary samples and generate a platform to evaluate the tumoricidal efficacy of autologous adoptive cell transfer including tumor infiltrating lymphocytes and peripheral blood lymphocytes.

**Methods:** Haematoxylin and eosin together with immunohistochemistry staining were employed to ascertain the morphologic and histological features of tumoroids and original tumors. Tumor killing ability of T cells was detected by lactate dehydrogenase assay and propidium iodide staining. In tumoroid xenograft mouse model, tumor volumes were measured and T cell functions were examined by flow cytometry technique.

**Results:** Four tumoroids with characteristics of poor differentiation and mild fibrosis were successfully established from fourteen hepatocellular carcinoma samples. More robust antitumor potential and hyper-functional phenotype of all four tumor infiltrating lymphocytes were observed compared to matched peripheral blood lymphocytes in coculture system. In tumoroid xenograft mouse models, however, only one patient-derived tumor infiltrating lymphocytes with the highest antitumor activity can bestow efficient tumor eradication.

**Conclusions:** Hepatocellular carcinoma tumoroid-based models could represent invaluable resources for evaluating the tumoricidal efficacy of autologous adoptive cell transfer. Tumor infiltrating lymphocytes should be a promising and yet-to-be-developed regimen to treat hepatocellular carcinoma.

**Keywords:** Hepatocellular carcinoma (HCC); tumoroid; tumor infiltrating lymphocytes; adoptive cell transfer treatment

Submitted Oct 31, 2021. Accepted for publication Mar 17, 2022.
doi: 10.21037/jgo-21-715
**View this article at:** https://dx.doi.org/10.21037/jgo-21-715

^ ORCID: 0000-0003-1731-5941.

## Introduction

Primary liver cancer is the fourth leading etiology of cancer-related mortality worldwide, causing nearly 740,000 deaths each year (1). Of these, hepatocellular carcinoma (HCC) constitutes about 75–85% of cases (2). In spite of hepatectomy being the optimal therapeutic option, it is challenging to meet the conditions of surgery for the moderate and advanced-stage HCCs. Furthermore, multi-kinase inhibitors and the immune-checkpoint inhibitors have been proven to modestly extend overall survival of patients (3,4). Given these unmet clinical needs, a highly encouraging immunotherapeutic strategy against tumor, adoptive cell therapy (ACT) using tumor-infiltrating lymphocytes (TILs) is under development in HCC (5).

Despite well-appreciated clinical benefits in metastatic melanoma and advanced cervical cancer (6,7), efficacy of TILs is still sub-optimal in HCC because of the limited tumor-specific T cell repertoire and technical difficulties in isolating and expanding those cells on an individual basis (8). Hence, it is crucial to select patients who might respond to treatment for improving clinical outcomes and optimizing processing protocols. To this end, two types of patient-derived models were developed to recapitulate the pathophysiology of the primary tumors and interactions with the immune system (9). One is tumor xenograft model in immunodeficient mice, which was described to more reliably mirror the physiology of individual tumor but it is costly and time-consuming (10). Whereas *in vitro* culture of primary tumor cells has been utilized as the main preclinical model to assess the treatment effects due to its easy-to-use and relative fidelity to original tumors. However, lack of sustained expansion, inadequate preservation of tumoral heterogeneity and the spatial interactions with the immune system have undermined its broad implementation (11,12).

Thus, tumoroid, a three-dimensional (3D) culture system of primary tumor cells growing along extracellular matrix scaffold (13), was developed from organoid (14) which can recapitulate an organ in 3D culture owing to the self-renewal and differentiation capacities for a longer growth and more faithful replication of the tumor heterogeneity and microenvironment compared to conventional 2D construct (15,16). On this ground, coculture of tumoroids with autologous peripheral blood lymphocytes (PBLs) were used as a platform to enrich tumor-reactive T cells and to estimate their tumoricidal activities against colorectal cancer and non-small cell lung cancer (17). Further, after coculture with matched tumoroids, the $CD39^{+}CD8^{+}$ subset of HCC-derived TILs was identified to present a better antitumor activity than $CD39^{-}CD8^{+}$ TILs (18). But the functional comparison between TILs and PBLs against tumoroid have never been characterized.

In current study, we incorporated autologous TILs or PBLs into tumoroids from HCC patients and found that TILs acquired higher degree of activated phenotype and more potent ability to eliminate HCCs compared to PBLs (*Figure 1*), suggesting that tumoroid is a viable assessment model and TILs should be exploitable to treat HCC. We present the following article in accordance with the ARRIVE and MDAR reporting checklists (available at https://jgo.amegroups.com/article/view/10.21037/jgo-21-715/rc).

## Methods

### *Animals and patients*

NOD/ShiLtJGpt-Prkdc$^{em26}$Il2rg$^{em26}$/Gpt (NCG) mice were purchased from GemPharmatech and maintained

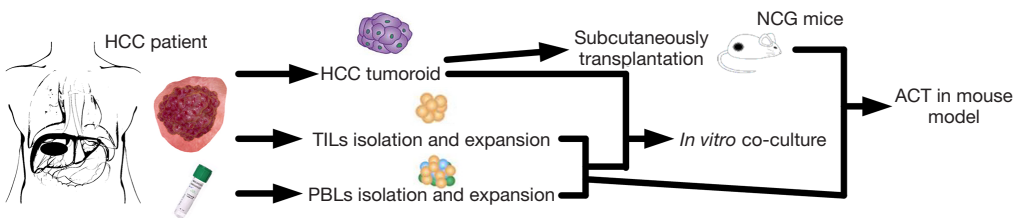


**Figure 1** Flow chart of the experimental design and analysis. HCC tumor tissue collected at the time of resection was used to establish tumoroid and to develop TIL cultures. Meanwhile, blood sample was isolated of PBLs which were then expanded. *In vitro* coculture system was assembled of tumoroid and matched TILs or PBLs. To establish tumoroid xenograft model, tumoroids was transplanted subcutaneously into the NCG mice. Afterwards, expanded TILs or PBLs were transferred intravenously into these models to study therapeutic efficacy. ACT, adoptive cell therapy; HCC, hepatocellular carcinoma; NCG, NOD/ShiLtJGpt-Prkdce$^{m26}$Il2rge$^{m26}$/Gpt; PBLs, peripheral blood lymphocytes; TILs, tumor-infiltrating lymphocytes.

 

**Table 1** Clinical and pathologic features of the HCC cohort categorized by the establishment of tumoroids

| No. | Sex | Age (years) | Edmondson grade | Etiology | ALBI grade | Ishak score | AFP (ng/mL) | Growth pattern | Tumor size (mm × mm) | Tumoroids |
|---|---|---|---|---|---|---|---|---|---|---|
| 1 | M | 57 | III | HBV | 1 | 3 | 413 | Solid | 97×73, 25×22 | Yes |
| 2 | M | 64 | III | HBV | 1 | 3 | 3,700 | Solid-trabecular | 29×17 | Yes |
| 3 | M | 67 | III | HBV | 1 | 4 | 3,479 | Solid-trabecular | 23×17 | Yes |
| 4 | M | 63 | III | HBV | 2 | 2 | 218 | Solid | 31×19 | Yes |
| 5 | M | 51 | III | HBV, ALD | 2 | 5 | 20,053 | Solid-trabecular | 68×71 | No |
| 6 | F | 46 | I | HBV | 1 | 4 | 498 | Solid | 63×31 | No |
| 7 | M | 42 | II | HBV | 2 | 2 | 32,727 | Solid | 95×70, 17×15 | No |
| 8 | M | 68 | II | HBV | 1 | 4 | 2,465 | Trabecular | 73×42 | No |
| 9 | M | 46 | III | HBV | 1 | 5 | 4,164 | Solid-trabecular | 91×64, 20×16 | No |
| 10 | M | 54 | II | ALD | 1 | 4 | 13.4 | Solid-pseudoglandular | 44×39 | No |
| 11 | M | 58 | II | HBV | 1 | 4 | 213 | Solid-trabecular | 79×30 | No |
| 12 | M | 59 | II | HBV | 1 | 5 | 1.19 | Solid | 21×17 | No |
| 13 | M | 60 | III | Unknown | 2 | 2 | 153 | Solid-trabecular | 54×32, 22×13 | No |
| 14 | M | 61 | II | HBV | 1 | 3 | 5.11 | Solid | 29×21 | No |

ALBI, albumin-bilirubin; AFP, α-fetoprotein; HCC, hepatocellular carcinoma; HBV, hepatitis B virus; ALD, alcoholic liver disease.

under specific pathogen-free conditions at the Laboratory Animal Services of Peking University First Hospital. The experimental protocol was approved by the Ethics Committee of Peking University First Hospital (the license number: LA2019194), in compliance with Peking University guidelines for the use of clinical samples and the care of animals. This protocol was prepared before the study without registration.

HCC specimens and blood samples were taken from fourteen patients with HCC who underwent liver resection in Beijing Cancer Hospital. All patients were first diagnosed of HCC following the guidelines for diagnosis and treatment of primary liver cancer in China (19) and had not yet received therapy. No disseminated metastasis was found in all patients. The detailed patients' data and clinicopathologic features of tumors were shown in *Table 1*. The study was conducted in accordance with the Declaration of Helsinki (as revised in 2013). The project has acquired the informed consents from patients and ethical approval from Beijing Cancer Hospital Ethics Committee (the license number: 2019KT14). The HCC specimen from each patient was cut into two pieces, one was digested for TIL culture and the other was processed for tumoroid construction.

### *In vitro expansion of TILs and PBLs*

HCC specimens were grinded and digested in T cell expansion medium (StemCell, Vancouver, Canada) with 30 U/mL DNaseI (Sigma-Aldrich, St. Louis, USA) and 1.0 mg/mL collagenase D (Roche, Basel, Switzerland) and incubated for 1 hour at 37 ℃. Meanwhile, paired peripheral blood mononuclear cells (PBMCs) were isolated by Ficoll-Paque (GE Biosciences, New York, USA) according to the manufacturer's manual. After wash and centrifugation, TILs and PBLs were cultured in T cell expansion medium supplemented with 600 IU/mL of recombinant human interleukin-2 (IL-2) (PeproTech, Rocky Hill, USA) and 25 ng/mL of anti-human CD3/CD28 (StemCell Technologies Cat# 10971, RRID:AB_28278, Vancouver, Canada) at 37 ℃ with 5% $CO_2$ for 2 weeks (17,20). Then cells were cocultured with irradiated allogeneic PBMCs isolated by Ficoll-Paque as feeders at a ratio of 1:100 in T cell expansion medium and IL-2 for 7–10 days. The quantity of TILs and PBLs were counted every 2 days.

### *Tumoroid culture*

Remaining HCC specimens were cut into small pieces and digested in EBSS (Life Technologies, Waltham, USA)

 

supplemented with 2.5 mg/mL collagenase D (Roche, Switzerland) and 0.1 mg/mL DNaseI (Sigma-Aldrich, USA) for about 1 hour at 37 ℃. After centrifugation, the HCCs pellet were embedded in Basement Membrane Extract Type2 (BME2, R&D Systems, Minneapolis, USA) for 20 minutes at 37 ℃ and were resuspended in human HCC organoid medium composed of Advanced DMEM/F12 supplemented with 1% Glutamax (Life Technologies, USA), 10 mM HEPES (Sigma-Aldrich, USA), 1:50 B27 supplement (without vitamin A) (Life Technologies, USA), 1:100 N2 supplement (Sigma-Aldrich, USA), 1.25 mM N-acetyl-l-cysteine (Sigma-Aldrich, USA), 10% Rspo-1 conditioned medium (PeproTech, USA), 30% Wnt3a-conditioned medium (JSR, Tokyo, Japan), 10 mM nicotinamide (Sigma-Aldrich, USA), 10 nM recombinant human (Leu15)-gastrin I (Sigma-Aldrich, USA), 50 ng/mL recombinant human epidermal growth factor (EGF) (PeproTech, USA), 100 ng/mL recombinant human fibroblast growth factor 10 (FGF10) (PeproTech, USA), 25 ng/mL recombinant human hepatocyte growth factor (HGF) (PeproTech, USA), 10 μM forskolin (Tocris, Ellisville, USA), 5 μM A8301 (Tocris, USA), 25 ng/mL Noggin (PeproTech, USA) and 10 μM Y27632 (Sigma-Aldrich, USA) to establish tumoroids (21,22). The tumoroids were passaged every 1–2 weeks after dissociation with 0.25% trypsin (Gibco, Grand Isle, USA). For storage, the tumoroids were dissociated and resuspended in recovery cell culture freezing medium (StemCell, Canada) according to standard procedures.

### *Haematoxylin and eosin (H&E) and immunohistochemistry (IHC) staining*

Formalin-fixed and paraffin-embedded liver sections and tumoroids were processed for antigen retrieval with 10 mM sodium citrate. The tissue slides were blocked with 1% bovine serum albumin (BSA) (Sigma-Aldrich, USA) for 1 hour and incubated with following primary antibodies purchased from Origene: anti-cytokeratin19 (KRT19) (OriGene Cat# TA500018, RRID:AB_1528108, Rockville, USA), anti-epithelial cell adhesion molecule (EpCAM) (OriGene Cat# TA506627, RRID:AB_2623831, USA), anti-α-fetoprotein (AFP) (OriGene Cat# TA809081, RRID:AB_2629001, USA), anti-hepatocyte paraffin 1 (HepPar-1) in phosphate buffer saline (PBS) (Sigma-Aldrich, USA) and 1% BSA overnight at 4 ℃. Then the slides were washed five times with 0.5% PBS plus TWEEN-20 (PBST, Sigma-Aldrich, USA) and incubated with 1:1,000 diluted biotinylated secondary antibody for another hour. Slides were washed five times with 0.5% PBST and incubated with ABC solution. Tissues were visualized using AEC (DAKO, Santa Clara, USA), followed by Mayor's haematoxylin counterstaining. Eventually, images were captured with Nikon (TE2000-S) microscopes.

### *Lactate dehydrogenase (LDH) assay and propidium iodide (PI) staining*

After 6–8 months of expansion, part of tumoroids were dissociated into single cells and counted. Then 2,000 single cells from tumoroids were mixed with autologous TILs or PBLs or PBS at indicated effector/target (E/T) ratios. In some experiments, TILs and PBLs were sorted by anti-CD4 or anti-CD8 conjugated magnetic cell following the instruction of $CD4^+$ and $CD8^+$ T Cell Isolation Kit (StemCell, Canada). They were cultured in T cell expansion medium containing 600 IU/mL human IL-2 and anti-human CD3/CD28 after BME2 polymerization in triplicate wells from 24-well cell culture plates at 37 ℃ with 5% $CO_2$ (17,23). After 7 days, the media was extracted and the cytotoxicity of lymphocytes were determined by measuring the LDH activity according to the manufacturer's instructions (Promega, Madison, USA). On day 3 and day 7, the cells were stained with 25 mg/mL PI (BD Biosciences, San Jose, USA) for 30 minutes at 4 ℃, and immediately were imaged using a microscope camera. On day 7, the cells were dissociated with 0.25% trypsin and stained with 50% trypan blue (Sigma-Aldrich, USA) to count the cell number. Tumoroids alone cultured in the same medium with PBS supplement or TILs alone were cultured were used as the negative controls.

### *Autologous ACT in tumoroid xenograft mouse model*

For subcutaneous grafts, 1 million tumoroid cells were dissociated and suspended in PBS and subsequently were injected into left flanks of twenty female 2-month-old NCG mice. After 2–5 months, mouse with tumors volume reaching 150–200 $mm^3$ was randomly selected to be intravenously infused of $1\times10^7$ matched TILs or PBLs or PBS, or $1\times10^8$ TILs followed by 45,000 IU IL-2 was intravenously given daily for 3 days and then twice weekly. Each group comprised three mice. Tumor volumes were then measured by caliper every 5 days and peripheral blood was collected at different time points. When skin rupture happened or the tumor volume reached >500 $mm^3$, mice were euthanized according to guidelines.

 

### *Flow cytometry analysis*

On day 7 after coculture with tumoroids, TILs or PBLs were dissociated to single cells using trypsin. Since day 3 after adoptive transfer, lymphocytes from mouse peripheral blood were collected. They were stained with the following anti-human antibodies purchased from BioLegend: anti-CD3-FITC (BioLegend Cat# 317306, RRID:AB_571907, San Diego, USA), anti-CD39-APC (BioLegend Cat# 328210, RRID:AB_1953234, USA), anti-CD69-PE (BioLegend Cat# 310906, RRID:AB_314841, USA), anti-CD107a-APC-Cy7 (BioLegend Cat# 328630, RRID:AB_2562109, USA), anti-PD1-PE-Cy7 (BioLegend Cat# 621616, RRID:AB_2832836, USA), anti-CD62L-APC (BioLegend Cat# 304810, RRID:AB_314470, USA), anti-CD45RO-PE (BioLegend Cat# 304206, RRID:AB_314422, USA) and anti-mouse CD45-APC (BioLegend Cat# 147708, RRID:AB_2563540, USA) for 30 minutes at 4 ℃. Some cells were stimulated with 50 ng/mL phorbol 12-myristate 13-acetate (PMA) (InvivoGen, San Diego, USA) and GolgiStop (BD Biosciences, USA) for 4 hours at 37 ℃, then were fixed and washed using the Cytofix/Cytoperm plus Fixation/Permeabilization Solution kit (BD Biosciences, USA), finally were stained with anti-human interferon γ (IFN-γ)-APC (BioLegend Cat# 502512, RRID:AB_315237, USA) and anti-human tumor necrosis factor α (TNF-α)-PE (BioLegend Cat# 502909, RRID:AB_315261, USA). All cells were recorded using a FACS system (BD Biosciences FACS Celesta Flow Cytometer, RRID:SCR_019597, USA) and data were analyzed using FCS Express 6 software (De Novo Software, Pasadena, USA).

### *Statistical analysis*

Data were analyzed using Student's unpaired *t*-test, two-tailed Student's *t*-test and chi-square test with the Prism software (GraphPad Prism, RRID:SCR_002798, San Diego, USA), a P value of less than 0.05 was considered significant.

## Results

### *HCCs with poor differentiation and mild fibrosis are prone to establish tumoroids*

In an attempt to produce tumoroids, we collected HCC specimens from fourteen newly diagnosed patients. Most had been infected with hepatitis B virus (HBV) chronically except one with alcoholic liver disease (ALD) and one with unknown etiology. Serum test suggested that 11 patients (78.6%) over-represented AFP (≥10.9 ng/mL) in accordance with the survey outcomes to Chinese patients (24). According to an optimized operation protocol, four samples from HCC-1 to HCC-4 successfully generated tumoroids (*Table 1*, *Figure 2A*) and proliferated for more than half year in contrast to only one-month survival for conventional 2D culture. Correlation analysis of clinical and pathologic parameters indicated that the establishment success rate was mainly attributed to poor differentiation and mild cirrhosis of HCCs, wherein all tumoroids were derived from original tissues with Edmondson grade III while majority of unsuccessfully-produced samples (6/10, 60%) were classified into Edmondson grade II. At the fibrotic level, 75% (3/4) tumoroids were from original tissues with Ishak score below or at 3 compared to 70% (7/10) unaccomplished specimen with Ishak score at or above 4 (*Figure 2B*). Other features such as AFP serum levels, tumor size, etiology and growth pattern were nonetheless unlikely to affect the success rate of tumoroid establishment (*Figure 2C*, data not shown). To determine whether the tumoroids would retain the histological features of the patient-derived HCC tissues, hematoxylin and eosin (H&E) staining of paraffin-embedded sections showed that the tumoroids contained analogous cellular and histological architecture to the patient's tissue including heterogeneously-shaped, pseudo-stratified epithelium or cyst-like epithelial (*Figure 2D*). Further hallmark analysis of tumoroids suggested that half patients (2/4) expressed the poorly differentiated signature EpCAM and keratin 19 (KRT19), all samples (4/4) were AFP positive, yet none (0/4) expressed a well-differentiated marker HepPar-1, which demonstrated a poorly differentiated feature in line with the expression profile of the original patients' tissue (*Figure 2E*). In sum, these results suggested that HCCs with poor differentiation and mild fibrosis are prone to generate tumoroids maintaining the histological feature and biomarkers of the original tumor tissue, while the long-term expansion endows tumoroids with sufficient amounts and timescale for *in vitro* studies.

### *TILs obtain better anti-HCC activity against autologous tumoroids than PBLs*

To investigate whether TILs have the capability of tumor-killing, we isolated and expanded four matched TILs and PBLs and then cocultured with autologous tumoroids weekly to assess their cytotoxic efficiency. Using LDH release assay, we found that TILs generated much more

 

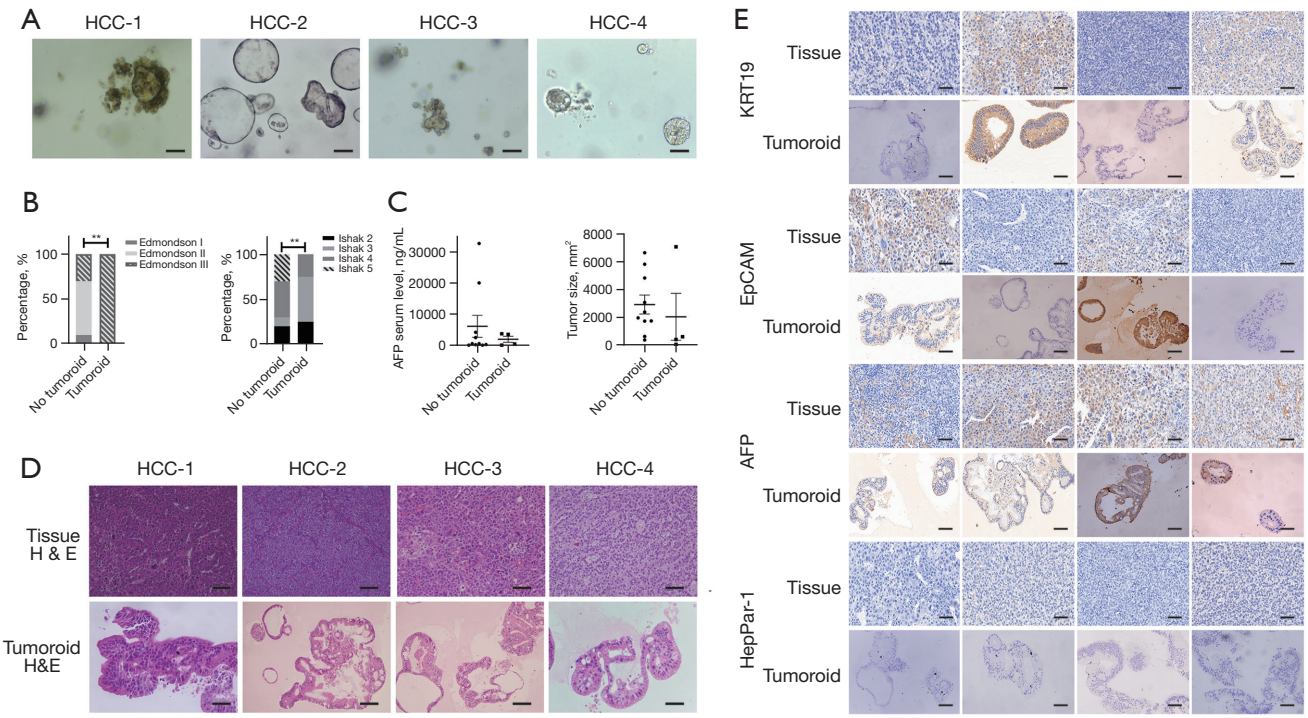


**Figure 2** HCC tumoroids are more achievable from samples with poorer differentiation plus milder fibrosis and maintain the pathologic profile of the original tumors. (A) Brightfield microscopy images of four tumoroids. Scale bars: 100 μm. (B) The bar graph compositing the percentage of patients with diverse Edmondson grade and Ishak score. (C) The dot graph showing AFP serum levels and HCC tumor sizes in tumoroids (tumoroids, n=4) and unsuccessfully-produced tumoroids (no tumoroids, n=10) groups. (D) Representative H&E staining of primary tumors (top row) and of the tumoroids derived from them (bottom row). Scale bars: top row, 100 μm; bottom rows, 50 μm. (E) IHC assays were performed using primary antibodies against KRT19, EpCAM, AFP, HepPar-1 overnight and then biotinylated secondary antibody for 1 hour in formalin-fixed and paraffin-embedded HCC sections and tumoroids. Finally, they were incubated with ABC solution and visualized using AEC. Original magnification, ×200. Scale bar: 100 μm. **, P<0.01. AFP, α-fetoprotein; EpCAM, epithelial cell adhesion molecule; HCC, hepatocellular carcinoma; HepPar-1, hepatocyte paraffin 1; KRT19, cytokeratin19.

potent cytotoxic effect against tumoroid cells than PBLs, one of which from HCC-3 patient even lacked tumor reactivity (*Figure 3A*). Concordantly, TILs underwent higher rate of propagation compared to PBLs (*Figure 3B*). Among them, TILs from HCC-2 manifested the highest propagation rate as well as most potent killing effect which was dose-dependent and detectable even at an E/T ratio as low as 5 (*Figure 3C*). PI staining also validated an increasing number of dead cells after exposed to this TILs than to PBLs in both 3 and 7 days of coculture (*Figure 3D*). Further analysis of the tumoricidal subset revealed a dominant cytotoxic role of $CD8^+$ T cells rather than $CD4^+$ T cells (*Figure 3E*). This potent antitumor function of TILs inspired us to examine their phenotypes. With regard to activation state, although the percentages of $CD39^+$ and $CD69^+$ were similar between matched TILs and PBLs from HCC-2 upon *in vitro* expansion, the levels of both markers were substantially elevated from TILs over PBLs after 1 week of coculture with tumoroids. This process also functionalized TILs with more degranulation marker CD107a expression and proinflammatory cytokine IFN-γ secretion than PBLs. Meanwhile, TILs obtained a more exhausted state with higher programmed death 1 (PD-1) expression. However, TILs and PBLs were indistinguishable to assume an effector memory phenotype with similar levels of CR45RO and CD62L expression before and after cocultivation with tumoroids. While only CD39 instead of CD69, CD107a and IFN-γ expression increased in TILs from HCC-2 than from another three patients after coculture with tumoroids (*Figure 3F*). Therefore, these data showed that despite the analogous phenotype of paired TILs and PBLs in response to *in vitro* unspecific CD3/

 

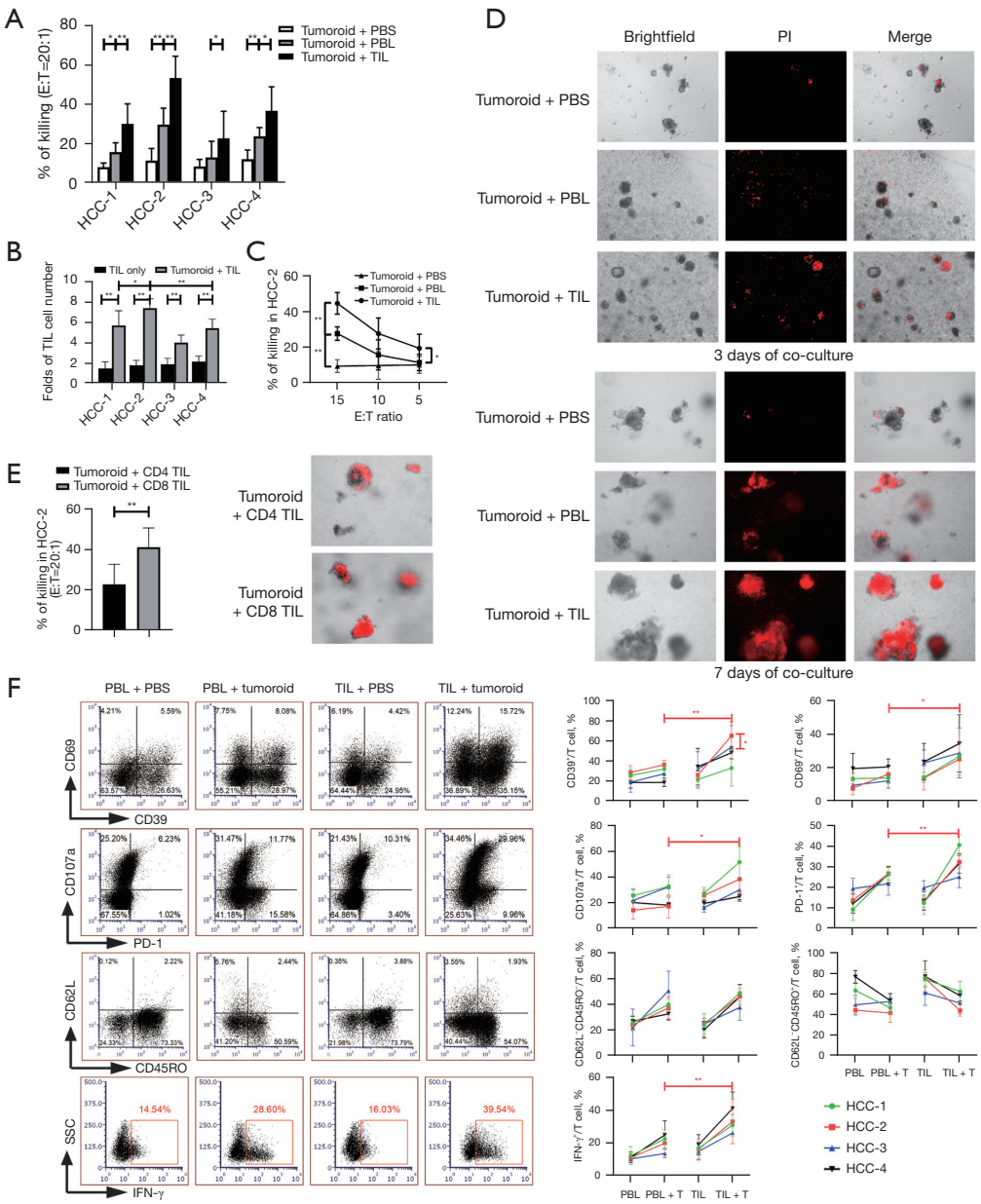


**Figure 3** TILs generate activation state and cytotoxicity against *in vitro* cultured autologous tumoroids. TILs or PBLs or PBS was added into tumoroids in triplicate wells. (A) The killing efficacy was measured by LDH assay. (B) The number of TILs was quantified and the fold increase against the number on day 0 was shown after 7 days of culture without or with tumoroids at 20 of E/T ratio from 4 HCC patients. (C) The killing efficacy was measured at serial E/T ratios from HCC-2 patient after 7 days of coculture. (D) Dead tumoroids were visualized by PI staining after 3- and 7-day coculture with TILs and PBLs. Magnification, ×200. (E) The cytotoxic effects of $CD4^+$ and $CD8^+$ TILs were detected by LDH assay and PI staining after 7 days of coculture at 20 of E/T ratio from HCC-2 patient. Magnification, ×200. (F) Representative dot plots show the percentages of CD39, CD69, CD107a, PD-1, CR45RO, CD62L expressing and IFN-γ producing cells after PMA stimulation gated on $CD3^+$ T cells on the 7th day post-coculture. A summary of 4 patients is depicted by line graphs. The capped line denotes the comparison of HCC-2. Tumoroids or TILs were cultured with PBS supplement as negative controls. These experiments were repeated with similar data. *, P<0.05; **, P<0.01. E/T, effector/target; HCC, hepatocellular carcinoma; IFN-γ, interferon γ; LDH, lactate dehydrogenase; PBLs, peripheral blood lymphocytes; PBS, phosphate buffer saline; PD-1, programmed death 1; PI, propidium iodide; SSC, side scatter; TILs, tumor-infiltrating lymphocytes.

 

CD28 antibodies plus IL-2 stimulation, TILs obtained more potent cytotoxic activity against autologous tumoroids mediated by direct killing effect and proinflammatory cytokines production.

### *Only TILs with the highest antitumor reactivity show tumor-destructive ability in autologous tumoroid xenograft mouse models*

Following *in vitro* evaluation of anti-HCC potential of TILs and PBLs, we sought to dissect them in autologous tumoroid xenograft mouse models. Firstly, we injected four tumoroids subcutaneously into NCG immunodeficiency mice to model the features of original HCC tissues. When the tumors volume reached 150–200 $mm^3$, we infused autologous TILs or PBLs to investigate their antitumor effects. Surprisingly, only TIL from HCC-2 with the most highly reactive to tumoroid could almost eliminate it while other three TILs and all four PBLs barely influenced tumor progression (*Figure 4A*). The proliferation capacity of transferred lymphocytes also correlated with antitumor efficacy, wherein only TIL from HCC-2 was identified in peripheral blood as early as three days and as long as 7 weeks post-transfer in contrast to sustained lack of transferred cells from other patients indicated by HCC-1 as a paradigm (*Figure 4B*). Similar tumor growth trajectories and percentages of peripheral TILs to murine PBMCs were identified even following the infusion of ninefold more TILs to $1\times10^8$ each mouse (data not shown). On week three post-transfer corresponding to the peak of proliferation rates (*Figure 4B*), flow cytometric analysis of this TILs also demonstrated both proinflammatory cytokines TNF-α and IFN-γ secretion was upregulated, as was the exhausted marker PD-1 after its adoptive transfer. However, unlike *in vitro* coculture scenario, the percentages of CD45RO were reduced, representing a conversion from effector memory to effector subtype (*Figure 4C*).

## Discussion

The term "organoid" refers to a novel 3D culture systems with improved reminiscence of the characteristics and functions of mammalian tissues (25). On this ground, the tumoroid was created to model the genetic complexity and long-term growth of tumor (12). Based on the previous HCC-derived tumoroid manufacture protocol (21), We convincingly produced four tumoroids derived from fourteen individuals with HCC and continuously cultured beyond half year. Although the success rate closely resembles previous reports regarding HCC tumoroids establishment (15), this low efficiency (29%) prompted us to analyze the underlying causes. Among all clinical and pathological features, poor tumor differentiation and slight cirrhosis turn out to favor the generation of tumoroids likely because poorly differentiated HCCs might lead to a greater proliferation capacity and milder fibrotic tissues enable easier digestion and more tumor cells yield (9). To demonstrate whether tumoroids faithfully maintain parental tumor features, we performed H&E and IHC staining of paraffin-embedded sections. At the histological level, tumoroids presented parental HCCs-coherent heterogeneous morphologies, such as compact rosettes, pseudo-stratified layers and cyst-like structures. Biomarker visualization suggested the shared expression profile of the tumoroids and parental tumors. In addition, it also supported that tumoroids mainly were derived from poorly differentiated HCCs because tumoroids with EpCAM or KRT19 expressing are more prevalent than those with well-differentiated hallmark HepPar-1 expression (21).

After establishing tumoroids successfully, we next employed it to assess the PBL and TIL killing efficacy. The more multi-antitumor specific TCR clonotypes and superior tumor-homing ability favor TIL in treating solid tumors compared with matched PBL and other ACTs (26). Nevertheless, the de facto application of TIL therapy currently is still limited in several kinds of tumors (27). For HCC, lack of tumor-reactive clones in the repertoire of TILs and technical difficulties in isolating and expanding these cells could be the major reasons for its application restraint (28). To interrogate whether TIL and PBL carry tumoricidal ability and afford therapeutic potential for HCC patients, we set HCC-derived tumoroids as target and cocultured them with TIL or PBL. Analogous to the previous report concerning ovarian cancer (29), *in vitro* killing assay suggested that TIL gives rise to more robust antitumor responses, simultaneously acquiring highly activated phenotype and cytotoxic function together with the more exhaustive propensity compared to PBL (30). With respective to the relationship of anti-tumor ability and immune phenotype of TILs, although HCC-2 presented the highest levels of tumoroid reactivity, only CD39 instead of CD69, CD107a and IFN-γ expression increased presumably owing to other tumor killing mechanisms.

We then exploited their antitumor function *in vivo* by tumoroid xenograft mouse models. As with tumoroids, patient-derived xenograft (PDX) mouse models are also described to be able to recapitulate the intra- and inter-

 

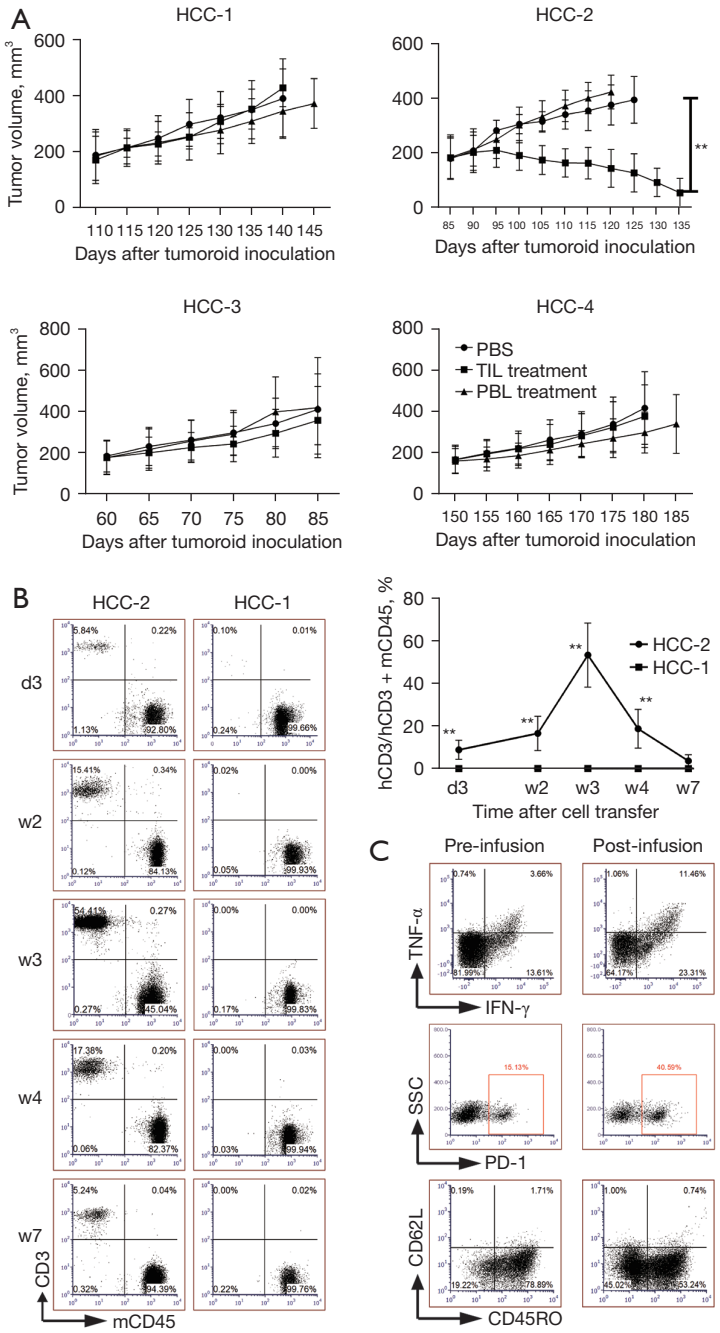


**Figure 4** Only TILs with the highest antitumor ability can inhibit tumor growth in autologous tumoroid xenograft mouse models. TILs or PBLs from four patients or PBS were injected into 3 mouse models each group as tumor volumes reached 150–200 $mm^3$. (A) The tumor growth curve is shown. (B) Representative dot plots display the human $CD3^+$ and $mCD45^+$ cells in peripheral blood mononuclear cells on 3rd day (d3), 2nd week (w2), w3, w4, w7 post-adoptive transfer of TILs from HCC-2 and HCC-1 patients. The line graph summarizes the proportion of transferred $CD3^+$ cells among peripheral mononuclear cells composed of $hCD3^+$ and $mCD45^+$ cells (n=3). (C) Representative dot plots suggest the percentages of PD-1, CR45RO, CD62L expressing and TNF-α plus IFN-γ secreting cells after PMA stimulation of peripheral human $CD3^+$ T cells from HCC-2 patient on pre-infusion and 3 weeks post-infusion. **, P<0.01. HCC, hepatocellular carcinoma; hCD3, human CD3; IFN-γ, interferon γ; mCD45, murine CD45; PBLs, peripheral blood lymphocytes; PBS, phosphate buffer saline; PD-1, programmed death 1; PMA, phorbol 12-myristate 13-acetate; SSC, side scatter; TILs, tumor-infiltrating lymphocytes; TNF-α, tumor necrosis factor α.

 

tumor heterogenous microenvironment (31). Therefore, we combined both promising armaments (21) to confirm the feasibility of TIL or PBL therapy. Specifically, four tumoroids were transplanted under the skin of immunocompromised mice and the histological evidences suggested they still resembled the corresponding tumors after long-term growth. However, after transfer of autologous TILs or PBLs into NCG mice followed by high doses of IL-2 administration based on the protocol of melanoma PDX model treated with TILs (32), which also models clinical trial settings composed of lymphodepletion and IL-2 infusion (33), only one TIL with the highest reactivity against tumoroid could be detected in periphery and implicated the curative role, even with 10 times the reported amount (29), suggesting cellular function instead of quantity determines the therapeutic outcome. However, the underpinning mechanism requires further investigation. As above, the *in vitro* and *in vivo* lytic ability against tumoroids came to coincident results, as did elevated activation and exhaustion properties of TILs. In spite of the significant antitumor efficacy *in vitro*, *in vivo* application prospect is unsatisfactory probably because direct contact of effector T cells with targeted tumor and T cell expansion medium facilitate the killing role (17) contrary to the complex and segregated environment likely requiring more functional T cells *in vivo*, which might also be the reason why curative effect was achieved exclusively upon cotreatment with checkpoint inhibitors (29). Furthermore, it is advisable to confirm these findings in a larger number of cases afterwards.

## Conclusions

This is the first study that reports the utilization of HCC tumoroid in evaluating the tumoricidal outcomes of paired TIL and PBL from patients. *In vitro* co-cultivation assay demonstrated all TILs presented superior antitumor activity relative to PBLs, but only one with the most potent lytic activity could reduce the tumor burden after infusion into tumoroid xenograft mouse models, which might highlight the necessity to increase cytolytic or stem-like function or tumor-directed specificity of transferred cells to yield clinical benefit.

## Acknowledgments

The authors acknowledge Dr. Shenshen Kong and staffs in the animal facility for assistance with experiments.

*Funding:* This work was supported by the Natural Science Foundation of Beijing Municipality (grant number 7162190) and the National Natural Science Foundation of China (grant numbers 81572808 and 81773252). This work was also supported by Joint Institute of Michigan Medicine and Beijing University Health Science Center.

## Footnote

*Reporting Checklist:* The authors have completed the ARRIVE and MDAR reporting checklists. Available at https://jgo.amegroups.com/article/view/10.21037/jgo-21-715/rc

*Data Sharing Statement:* Available at https://jgo.amegroups.com/article/view/10.21037/jgo-21-715/dss

*Conflicts of Interest:* All authors have completed the ICMJE uniform disclosure form (available at https://jgo.amegroups.com/article/view/10.21037/jgo-21-715/coif). The authors have no conflicts of interest to declare.

*Ethical Statement:* The authors are accountable for all aspects of the work in ensuring that questions related to the accuracy or integrity of any part of the work are appropriately investigated and resolved. The study was conducted in accordance with the Declaration of Helsinki (as revised in 2013). The project has acquired the informed consents from patients and ethical approval from Beijing Cancer Hospital Ethics Committee (the license number: 2019KT14). The experimental protocol was approved by the Ethics Committee of Peking University First Hospital (the license number: LA2019194), in compliance with Peking University guidelines for the use of clinical samples and the care of animals. The protocols including the research questions, key design features, and analysis plan were prepared before the study but without registration.

## References


1. Bray F, Ferlay J, Soerjomataram I, et al. Global cancer statistics 2018: GLOBOCAN estimates of incidence and mortality worldwide for 36 cancers in 185 countries. CA Cancer J Clin 2018;68:394-424.
2. Singal AG, Lampertico P, Nahon P. Epidemiology and surveillance for hepatocellular carcinoma: New trends. J Hepatol 2020;72:250-61.
3. Finn RS, Qin S, Ikeda M, et al. Atezolizumab plus Bevacizumab in Unresectable Hepatocellular Carcinoma. N Engl J Med 2020;382:1894-905.
4. Lee KH, Lee MS. Atezolizumab plus bevacizumab for unresectable hepatocellular carcinoma - Authors' replys. Lancet Oncol 2020;21:e413.
5. Rosenberg SA, Restifo NP. Adoptive cell transfer as personalized immunotherapy for human cancer. Science 2015;348:62-8.
6. Wang S, Sun J, Chen K, et al. Perspectives of tumor-infiltrating lymphocyte treatment in solid tumors. BMC Med 2021;19:140.
7. Zacharakis N, Chinnasamy H, Black M, et al. Immune recognition of somatic mutations leading to complete durable regression in metastatic breast cancer. Nat Med 2018;24:724-30.
8. Hendrickson PG, Olson M, Luetkens T, et al. The promise of adoptive cellular immunotherapies in hepatocellular carcinoma. Oncoimmunology 2020;9:1673129.
9. Bresnahan E, Ramadori P, Heikenwalder M, et al. Novel patient-derived preclinical models of liver cancer. J Hepatol 2020;72:239-49.
10. Zhu M, Li L, Lu T, et al. Uncovering Biological Factors That Regulate Hepatocellular Carcinoma Growth Using Patient-Derived Xenograft Assays. Hepatology 2020;72:1085-101.
11. Tharehalli U, Svinarenko M, Lechel A. Remodelling and Improvements in Organoid Technology to Study Liver Carcinogenesis in a Dish. Stem Cells Int 2019;2019:3831213.
12. Finnberg NK, Gokare P, Lev A, et al. Application of 3D tumoroid systems to define immune and cytotoxic therapeutic responses based on tumoroid and tissue slice culture molecular signatures. Oncotarget 2017;8:66747-57.
13. Lewis K, Takebe T. Tumoroid à la carte: Path for personalization. Hepatology 2018;68:1189-91.
14. Sato T, Vries RG, Snippert HJ, et al. Single Lgr5 stem cells build crypt-villus structures in vitro without a mesenchymal niche. Nature 2009;459:262-5.
15. Nuciforo S, Fofana I, Matter MS, et al. Organoid Models of Human Liver Cancers Derived from Tumor Needle Biopsies. Cell Rep 2018;24:1363-76.
16. Bar-Ephraim YE, Kretzschmar K, Clevers H. Organoids in immunological research. Nat Rev Immunol 2020;20:279-93.
17. Dijkstra KK, Cattaneo CM, Weeber F, et al. Generation of Tumor-Reactive T Cells by Co-culture of Peripheral Blood Lymphocytes and Tumor Organoids. Cell 2018;174:1586-1598.e12.
18. Liu T, Tan J, Wu M, et al. High-affinity neoantigens correlate with better prognosis and trigger potent antihepatocellular carcinoma (HCC) activity by activating CD39+CD8+ T cells. Gut 2021;70:1965-77.
19. Department of Medical Administration, National Health and Health Commission of the People's Republic of China. Guidelines for diagnosis and treatment of primary liver cancer in China (2019 edition). Zhonghua Gan Zang Bing Za Zhi 2020;28:112-28.
20. Jin J, Sabatino M, Somerville R, et al. Simplified method of the growth of human tumor infiltrating lymphocytes in gas-permeable flasks to numbers needed for patient treatment. J Immunother 2012;35:283-92.
21. Broutier L, Mastrogiovanni G, Verstegen MM, et al. Human primary liver cancer-derived organoid cultures for disease modeling and drug screening. Nat Med 2017;23:1424-35.
22. Broutier L, Andersson-Rolf A, Hindley CJ, et al. Culture and establishment of self-renewing human and mouse adult liver and pancreas 3D organoids and their genetic manipulation. Nat Protoc 2016;11:1724-43.
23. Takashima S, Martin ML, Jansen SA, et al. T cell-derived interferon-γ programs stem cell death in immune-mediated intestinal damage. Sci Immunol 2019;4:eaay8556.
24. Prospective suRveillance for very Early hepatoCellular cARcinoma(PreCar) expert panel. Expert consensus on early screening strategies for liver cancer in China. Zhonghua Gan Zang Bing Za Zhi 2021;29:515-22.
25. Huch M, Koo BK. Modeling mouse and human development using organoid cultures. Development 2015;142:3113-25.
26. Paijens ST, Vledder A, de Bruyn M, et al. Tumor-infiltrating lymphocytes in the immunotherapy era. Cell Mol Immunol 2021;18:842-59.
27. Geukes Foppen MH, Donia M, Svane IM, et al. Tumor-infiltrating lymphocytes for the treatment of metastatic cancer. Mol Oncol 2015;9:1918-35.
28. Ma W, Wu L, Zhou F, et al. T Cell-Associated Immunotherapy for Hepatocellular Carcinoma. Cell


 

Physiol Biochem 2017;41:609-22.
29. Gitto SB, Kim H, Rafail S, et al. An autologous humanized patient-derived-xenograft platform to evaluate immunotherapy in ovarian cancer. Gynecol Oncol 2020;156:222-32.
30. Pedersen M, Westergaard MCW, Milne K, et al. Adoptive cell therapy with tumor-infiltrating lymphocytes in patients with metastatic ovarian cancer: a pilot study. Oncoimmunology 2018;7:e1502905.
31. Yan HHN, Siu HC, Law S, et al. A Comprehensive Human Gastric Cancer Organoid Biobank Captures Tumor Subtype Heterogeneity and Enables Therapeutic Screening. Cell Stem Cell 2018;23:882-897.e11.
32. Jespersen H, Lindberg MF, Donia M, et al. Clinical responses to adoptive T-cell transfer can be modeled in an autologous immune-humanized mouse model. Nat Commun 2017;8:707.
33. Creelan BC, Wang C, Teer JK, et al. Tumor-infiltrating lymphocyte treatment for anti-PD-1-resistant metastatic lung cancer: a phase 1 trial. Nat Med 2021;27:1410-8.

**Cite this article as:** Zhou Z, Yan X, Shi W, Tan K, Shao C, Wang Y, Wang G, Hong Y. Evaluation of the tumoricidal efficacy of adoptive cell transfer using hepatocellular carcinoma-derived organoids. J Gastrointest Oncol 2022;13(2):732-743. doi: 10.21037/jgo-21-715

 